UCRL- 82953
PREPRINT
CONF-791102--114

COMPUTER CODE DETERMINATION OF TOLERABLE ACCEL CURRENT AND VOLTAGE LIMITS DURING STARTUP OF AN 80 kV MFTF SUSTAINING NEUTRAL BEAM SOURCE

D. J. MAYHALL
R. D. ECKARD

This paper was prepared for submittal to
8th SYMPOSIUM ON ENGINEERING PROBLEMS OF
FUSION RESEARCH; IEEE; SHERATON HOTEL,
SAN FRANCISCO, CA., NOVEMBER 13-16, 1979

11-12-79

COMPUTER CODE DETERMINATION OF TOLERABLE ACCEL CURRENT AND VOLTAGE LIMITS DURING STARTUP OF AN 80 kV MFTF SUSTAINING NEUTRAL BEAM SOURCE

D. J. Mayhall and R. D. Eckard*
Lawrence Livermore Laboratory, Livermore, CA 94550

Summary

We have used a Lawrence Livermore Laboratory (LLL) version of the WOLF ion source extractor design computer code to determine tolerable accel current and voltage limits during startup of a prototype 80 kV Mirror Fusion Test Facility (MFTF) sustaining neutral beam source. Arc current limits are also estimated. The source extractor has gaps of 0.236, 0.721, and 0.155 cm. The effective ion mass is 2.77 AMU. The measured optimum accel current density is 0.266 A/cm^2. The gradient grid electrode runs at 5/6 V_a (accel voltage). The suppressor electrode voltage is zero for $V_a \leq 3$ kV and -3 kV for $V_a \geq 3$ kV. The accel current density for optimum beam divergence is obtained for $1 \leq V_a \leq 80$ kV, as are the beam divergence and emittance. The optimum steady pulse current density (0.285 A/cm^2, 78 A) is 7% above the measured optimum value. For $2.5 \leq V_a \leq 80$ kV, the optimum current density is always greater than predicted by the planar diode perveance relation. Allowable accel current density and voltage are determined for two types of beam divergence degradation about the optimum: incidence of the beam onto the suppressor electrode and a 30% increase in divergence. An allowed accel current-voltage parameter space for tolerable beam divergence is derived. Ranges of beam divergence are determined. The temporal variation of the allowed accel current-voltage parameter space is calculated versus arc current risetime from 20-200 μsec. The variation of the allowed parameter space is also calculated for various accel current-voltage delay times. This information is expected to be useful in designing of the Sustaining Neutral Beam Power Supplies.

Introduction

An LLL (Lawrence Livermore Laboratory) CDC 7600 version NEWWOLF4[1] of the Lawrence Berkeley Laboratory (LBL) WOLF[2,3] ion source extractor design computer code is used to determine tolerable accel current and voltage limits during startup of a prototype 80 kV MFTF sustaining neutral beam source.[4,5,6] This information is expected to be useful in the design and operation of the Sustaining Neutral Beam Power Supply System (SNBPSS).

Extractor Grid Configuration

The extractor grid electrodes are shown in Fig. 1, which shows optimized ion beam trajectories for accel voltages V_a of 1 and 80 kV. The electrode shapes are computational approximations to the actual shapes, which are more rounded. The entrance grid is triangular and has a rounded top. The gradient and exit grids are circular; the suppressor grid is teardrop-shaped. The entrance-gradient grid gap is 0.236 cm, the gradient-suppressor grid gap is 0.721 cm, and the suppressor-exit grid gap is 0.155 cm.

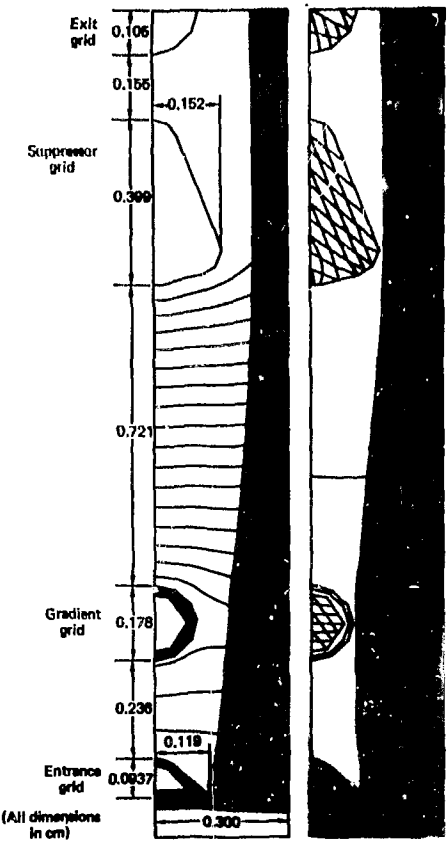

Fig. 1: Extractor Grid Configuration And Optimum Ion Beams For V_a = 80 kV and 1 kV

Assumed Plasma and Extractor Parameters

The potential at the plasma surface is taken as 30 V greater than that of the entrance grid. The ion

*Work performed under the auspices of the U.S. Department of Energy by the Lawrence Livermore Laboratory under contract number W-7405-ENG-48.

temperature is taken as 8.15 eV.[7] The effective ion mass is taken as 2.77 AMU, which corresponds to a species mixture of 67% O^+, 20% O_2^+, and 13% O_2^-. The plasma surface potential, ion temperature, and effective ion mass are constant for all computations. The gradient grid voltage is 5/6 V_a. The suppressor voltage is 0 for V_a < 3 kV and -3 kV for $V_a \geq 3$ kV, which is a specified SHIPPS operational mode. The desired electric field at the plasma surface is 300 V/cm. The measured optimum accel current density for this prototype is 0.266 A/cm^2 at 80 kV, which corresponds to an accel current I_a of 71 A.[8]

Optimization Procedure

At each investigated accel voltage, the plasma surface is made straight and placed at a trial position. The code is requested to move the surface to a shape and position for a surface electric field of 300 V/cm. Since previous experience has shown results to be fairly insensitive to the electric field value, fields between ~ 100 and 600 V/cm are taken as evidence of good surface optimization. Typical acceptable surfaces are shown in Fig 1.

Next, the plasma surface is fixed. The code is requested to vary the accel current density J_a for minimum rms beam divergence. If the surface E field stays in the acceptable range, the results of this optimization are taken as valid. In this manner, optimum accel current densities and beam divergences are obtained for V_a = 2.5, 10, 40 and 80 kV. At V_a = 1 kV, the optimum computed beam has trajectories which strike the gradient and suppressor grids. This result is rejected as conducive to sparkdown. Therefore, the accel current density is reduced by trial-and-error until the intermediate grids are just cleared. This beam is then defined as optimum for 1 kV. Figure 1 shows the trajectories for this 1 kV beam. $J_a = 2.23 \times 10^{-4}$ A/cm^2, which corresponds to I_a = 61.1 mA for the 10 by 45.6 cm entrance grid array at 60% transparency or 273.6 cm^2 free area. The rms divergence $\Delta\theta_{min}$ = 35.7 mradians.

Optimization is tried at V_a = 500 V, but the beam edge strikes the gradient grid for $1 \times 10^{-8} \leq J_a \leq 8.5 \times 10^{-5}$ A/cm^2 (2.7μA $\leq I_a \leq$ 23 mA). The plasma surface is always convex -- instead of concave, as desired. It may be necessary to change the desired surface E field for a focused beam at 500 V.

Computed Optimum Beam Results

Figure 2 shows optimum accel current density and accel current for V_a = 1, 2.5, 10, 40, and 80 kV. Estimated optimum arc currents I_{arc} are also shown. This estimation assumes a strictly linear relation between the accel and arc currents. The proportionality is taken as 1.5 arc A/accel A from experimental shot 8170, 1/19/79 at V_a = 88 kV, I_a = 80 A.[5] The crosses on Fig. 2 indicate the expected accel current from the planar diode relation with fixed electrode spacing and ion mass, i.e., $I_{a2} = I_{a1}(V_{a2}/V_{a1})^{1.5}$, normalized to the 78 A accel current optimum at 80 kV. The dots indicate the expected I_a for the same relation normalized to the measured current of 71 A at 80 kV. The larger difference between computed and planar diode values at 1 kV is probably due to redefinition of the optimum beam for intermediate grid clearance. The computed 80 kV optimum J_a (0.285 A/cm^2, 78 A) is 7.14% above the measured value (0.266 A/cm^2, 71 A). Measured accel current values from shots 7854 and 7857 of 1/18/79[5] are also shown in Fig. 2. Accurate measurements have not been made for V_a < 12 kV. The computed optimum rms beam divergence is shown in Fig. 3 vs V_a.

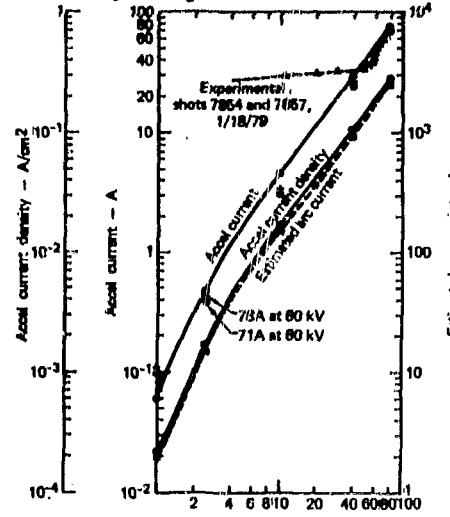

Fig. 2 Computed Optimum Currents and Accel Current Density

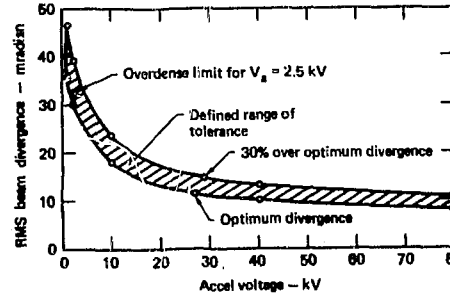

Fig. 3: Optimum RMS Divergence And Defined Range Of Tolerable Divergences

Determination of Tolerable Degradation in Divergence and Corresponding Accel Current

The maximum tolerable degradation in rms beam divergence is chosen as 30% of the optimum value $\Delta\theta_{min}$.[9] The tolerable divergence is thus $\Delta\theta_{max} = 1.3\Delta\theta_{min}$, which is shown in Fig. 3. Overdense

and underdense accel current densities which correspond to these divergence limits are determined at 10, 40, and 80 kV by trial-and-error trajectory evaluation. Underdense J_a limits are found similarly for 1 and 2.5 kV. The overdense limit for 2.5 kV is taken as the point of suppressor grid clearance, which is below $1.3\Delta\theta_{min}$. Because of the redefinition of the optimum beam for 1 kV, the overdense limit is the optimum beam. The corresponding accel current limits are shown in Fig. 4. Piecewise linear approximations to the accel current limits for $1 \leq V_a \leq 80$ kV are shown. The lower limit is extrapolated out to 85 kV. (The previous experimental values are also shown in Fig. 4.)

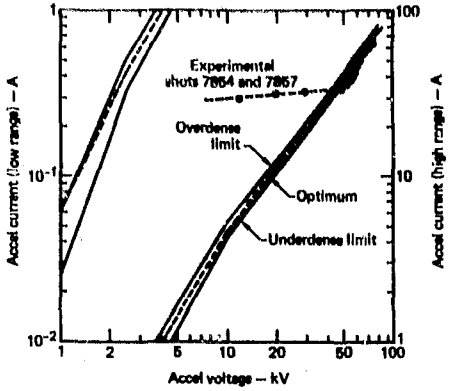

Fig. 4: Allowed Accel Current Versus Accel Voltage

The computed percent variation of the allowable accel current about the optimum is shown in Table 1. This variation is $\sim \pm 5\%$ at 80 kV and $\sim -60\%$ at 1 kV. The computed variation at 80 kV agrees qualitatively with the experimentally derived rule of thumb that the accel or arc currents can vary by about $\pm$ 10% for useful source operation.

Table 1

Variation of Allowable Accel Current About the Optimum

V_a (kV)	% Variation in I_a
80	+4.73, -5.10
40	+5.07, -7.06
10	+13.9, -7.61
2.5	+10.3, -29.2
1	+0, -58.9

Computed Variation of Allowed Accel Voltage With Arc Current Rise Time

In the planned scenario of source startup operation, the arc current is to be brought up to its desired steady pulse value 300 msec before V_a is applied across the extractor entrance and exit grids. Just before this application, I_{arc} is decreased or "notched" to a value $\geq$ 600 A. I_{arc} will then rise back up to its steady pulse value, as determined by the arc current notcher circuit and the arc chamber conditions. As I_{arc} rises, V_a is to be applied and properly controlled to produce an acceptably well focused beam during and after the arc current rise.

Fig. 4 is taken to constitute a computed approximate allowable I_a-V_a parameter space for tolerable source operation. It is used to determine the allowed range of V_a as I_{arc} rises to its steady pulse value at a constant rate. Given initial and final arc currents are chosen and the corresponding arc current rise rate dI_{arc}/dt is calculated for a given risetime τ_R. At succeeding times, I_a is calculated from the previously assumed linear relation. The corresponding accel voltage limits are then read from Fig. 4.

Example results are shown in Fig. 5 for $20 \leq \tau_R \leq 200\,\mu$sec. The arc current is notched to 600 A, the minimum presently specified for MFTF operation. It rises to 2535 A where I_a = 78 A. The initial allowed accel voltage range is 25.4-28.9 kV. Fig. 5 indicates that for proper source operation during beam startup, (i.e. correct I_a-V_a matching), the accel voltage, which is initially 0 at t = 0, must instantaneously jump into the allowed range. This is clearly impossible; some finite time is required for V_a to rise into the allowed band, after which it should rise at a slower rate with an acceptably focused beam.

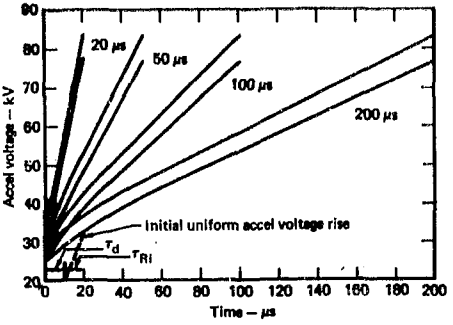

Fig. 5: Accel Voltage Limits Vs Risetime For 600 A Initial Arc Current

Experimental operation suggests the desirability of delaying the V_a rise with respect to the I_{arc} rise by up to tens of μsec. An example of a V_a waveform for a 10 μsec delay τ_d is shown in Fig. 5 by the dashed line. V_a rises uniformly to the minimum allowed value (32.5 kV) for τ_R = 200 μsec at 20 μsec after initiation. The initial V_a risetime τ_{RI} is 10 μsec.

Fig. 5 is used to calculate constant initial V_a rise rates to the allowed voltage bands for two delay times τ_d and initial V_a risetimes τ_{RI} from 2-80 μ sec. The arc current rise time τ_R = 100 μsec. Results are shown in Fig. 6. Bands of required initial dV_a/dt are shown at the bottom. The bands overlap as τ_{RI} exceeds 25 μsec. I_a at the time of V_a matching is shown at the top, as are the corresponding constant initial accel current rise rates.

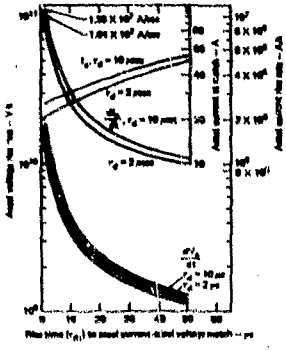

Fig. 6: Initial Constant Accel Voltage And Current Rise Rates For 100 μ Sec Arc Current Risetime

Conclusions

The experimental points in Fig. 4 show that the 80 kV source operates acceptably with an initial (V_a < 60 kV) V_a-I_a parameter space much wider than that predicted by the computations. The LBL Test Stand IIIB allowed a very rapid initial rise of I_{arc} and I_a, an initial V_a risetime of ~ 50 μsec, and a total V_a risetime of ~ 400 μ-sec. The computations should be repeated with the allowed divergence defined by incipient beam incidence onto the intermedite grids. A closer match between experiment and computation may then result.

Acknowledgements

Special thanks are due A. W. Molvik, T. J. Orzechowski, P. A. Willmann, and E. D. Baird.

References

1. P. A. Willmann, LLL, private communication, 1979
2. W. S. Cooper, K. Halbach, and S. B. Magyary, "Computer Aided Extractor Design," LBL, Berkeley, CA, LBL-3317, October, 1974
3. W. S. Cooper, and A. G. Paul, "WOLF A Computer Ion Beam Simulation Package," LBL, Berekley, CA, LBL-5373, August, 1974
4. A. W. Molvik, E. D. Baird, K. H. Berkner, W. S. Cooper, T. J. Duffy, K. H. Ehlers, J. Fink, D. Garner, and C. Wilder, "A Compact 80-keV Neutral-Beam Module," Proc. 7th Symposium Engineering Problems of Fusion Research, October, 1977, p. 295
5. A. W. Molvik, "Operation of 80 kV Neutral Beam," LLL SWOPSS Workshop, February 22, 1979
6. A. W. Molvik, "Testing of Developmental Neutral Beam Sources for MFTF", 8th Symposium on Engineering Problems Of Fusion Research, 1979, Paper 12-02
7. W. S. Cooper, LBL, private communication, 1979
8. A. W. Molvik, LLL, private communication, 1979
9. T. J. Orzechowski, LLL, private communication, 1979